



*Supplement of*

## **Above- and belowground plant mercury dynamics in a salt marsh estuary in Massachusetts, USA**

**Ting Wang et al.**

*Correspondence to:* Daniel Obrist ([daniel\\_obrist@uml.edu](mailto:daniel_obrist@uml.edu))

The copyright of individual parts of the supplement might differ from the article licence.

## 1 Supplementary Documents

### 2 Hg Isotope Mixing Model

3 We developed a ternary isotope mixing model to estimate the fractions of Hg in salt marsh plant leaves derived from the three  
4 dominant end-member Hg sources (medians). These sources include: (1) salt marsh plants roots, where the median Hg isotope  
5 composition of marsh plant roots collected in this study for  $\delta^{202}\text{Hg}$  is -0.69‰ (ranging from -0.75‰ to -0.66‰, n =4), for  $\Delta^{200}\text{Hg}$   
6 is 0.03‰ (ranging from -0.01‰ and 0.04‰), and for  $\Delta^{199}\text{Hg}$  is 0.17 ‰ (ranging from 0.11‰ to 0.22‰); (2) atmospheric GEM  
7 taken up by foliage, whereby we used published upland foliage Hg isotopic signatures that represent GEM taken up by plants from  
8 atmospheric GEM (on average 88% [79-100%, IQR]) of plant Hg is from GEM uptake (Zhou et al., 2021). The median Hg isotope  
9 compositions of upland foliage for  $\delta^{202}\text{Hg}$  is -2.84‰, for  $\Delta^{199}\text{Hg}$  is -0.37‰, and for  $\Delta^{200}\text{Hg}$  is -0.02‰ (n = 120) (review by Zhou  
10 et al., 2021); and (3) precipitation, where the median Hg isotope composition of precipitation is used from previous published data  
11 points ( $\delta^{202}\text{Hg}$ : -0.30‰,  $\Delta^{199}\text{Hg}$ : 0.4‰,  $\Delta^{200}\text{Hg}$ : 0.17‰ n = 106) (Table S6) (Jiskra et al., 2021). The calculation equations are as  
12 followings:

$$13 \Delta^{200}\text{Hg}_{vegetation} = f_{atm\_GEM}\Delta^{200}\text{Hg}_{atm\_GEM} + f_{root}\Delta^{200}\text{Hg}_{root} + f_{prep\_Hg(II)}\Delta^{200}\text{Hg}_{prep\_Hg(II)} \quad (1)$$

$$14 \delta^{202}\text{Hg}_{vegetation} = f_{atm\_GEM}\delta^{202}\text{Hg}_{atm\_GEM} + f_{root}\delta^{202}\text{Hg}_{root} + f_{prep\_Hg(II)}\delta^{202}\text{Hg}_{prep\_Hg(II)} \quad (2)$$

$$15 f_{atm\_GEM} + f_{root} + f_{prep\_Hg(II)} = 1 \quad (3)$$

16 To estimate and propagate uncertainty in the isotopic values reported in this study, we used Monte Carlo simulations (10,000 trials)  
17 to quantify the distribution of potential results (assuming a normal distribution), and we report the mean and standard deviation of  
18 results based on two calculation methods. The first method used the mean and standard deviation of observed  $\delta^{202}\text{Hg}$  and  $\Delta^{200}\text{Hg}$   
19 isotopic values for roots and vegetation to characterize uncertainty in the Monte Carlo simulations. The second method used the  
20 highest relative standard deviation recorded among analytical batches of certified reference materials (CRMs) to characterize  
21 uncertainty. Both methods yielded similar central results, suggesting approximately one-third contribution from each source.

### 22 Industrial Hg Isotopic Signatures

23 The isotopic signatures of industrial Hg are characterized by a wide range of negative  $\delta^{202}\text{Hg}$  values, while  $\Delta^{199}\text{Hg}$  and  $\Delta^{200}\text{Hg}$   
24 values are generally close to zero or positive (Fig S3, Table S4). For example, urban soil Hg signatures in Beijing, China showed  
25  $\delta^{202}\text{Hg}$  values between -1.14‰ and -0.59‰,  $\Delta^{199}\text{Hg}$  values between 0.03‰ and 0.10‰ and  $\Delta^{200}\text{Hg}$  values between 0.02‰ and  
26 0.04‰ (Huang et al., 2016); contaminated coastal marine sediments along Northeastern USA. showed  $\delta^{202}\text{Hg}$  values between -  
27 0.82‰ and -0.38‰,  $\Delta^{199}\text{Hg}$  values between 0.01‰ and 0.18‰ and  $\Delta^{200}\text{Hg}$  values between -0.04‰ and 0.02‰ (Kwon et al., 2014);  
28 industrial sources impacted sediments of Great Lakes USA showed  $\delta^{202}\text{Hg}$  values between -1.28‰ and -0.14‰,  $\Delta^{199}\text{Hg}$  values  
29 between -0.04‰ and 0.11‰ and  $\Delta^{200}\text{Hg}$  values between -0.02‰ and 0.09‰ (Lepak et al., 2015); and in Northeastern France  
30 showed  $\delta^{202}\text{Hg}$  values between -0.72‰ and -0.16‰ and  $\Delta^{199}\text{Hg}$  values between -0.08‰ and 0.09‰ (Estrade et al., 2011). Similarly,  
31 Hg isotopic signatures in historic industrial influenced bank soils of Virginia, USA, showed  $\delta^{202}\text{Hg}$  values between -1.05‰ and -  
32 0.18‰,  $\Delta^{199}\text{Hg}$  values between 0.00‰ and 0.10‰, and  $\Delta^{200}\text{Hg}$  values between -0.02‰ and 0.03‰ (Washburn et al., 2017).

33

34 **Table S1. Hg concentrations, dry weights, and Hg mass of above- and belowground biomass and surface soils of the two plant dominated**  
 35 **communities.**

Items	Plant species	Hg concentration $\mu\text{g kg}^{-1}$	STD	Dry Weight $\text{g m}^{-2}$	STD	Hg mass $\mu\text{g m}^{-2}$	STD
Live root	<i>S. alterniflorus</i>	84.5	47.0	278	61	22.0	7.9
	<i>S. pumilus</i>	258.9	70.3	444	87	118.0	53.8
Live rhizome	<i>S. alterniflorus</i>	27.9	1.1	598	44	18.8	3.5
	<i>S. pumilus</i>	46.6	14.2	987	87	57.4	2.9
Senesced biomass_0-20cm	<i>S. alterniflorus</i>	318.0	30.1	54	9	1912.3	606.3
	<i>S. pumilus</i>	323.3	135.4	6537	611	2068.0	1017.3
Mineral and humus_0-20cm	<i>S. pumilus</i>	272.3	11.6				
Bulk soil_0-20cm	<i>S. alterniflorus</i>	194.6	28.3	71078	6794	13925.8	3334.7
	<i>S. pumilus</i>	171.2	72.1	53193	10143	9470.1	5570.3
Senesced biomass_20-40cm	<i>S. alterniflorus</i>	639.1	337.1	2660	3704	3077.7	1512.2
	<i>S. pumilus</i>	263.1	208.7	5119	977	1174.2	845.2
Mineral and humus_20-40cm	<i>S. pumilus</i>	73.1	10.2				
Bulk soil_20-40cm	<i>S. alterniflorus</i>	279.1	203.8	70523	2904	19977.1	15183.1
	<i>S. pumilus</i>	159.1	122.7	55838	18002	7777.1	3986.2

36

37 Table S2. Hg concentrations, dry weights, and Hg mass of above- and belowground biomass and surface soils of the combined plant  
 38 communities.

	Items	Hg concentration $\mu\text{g kg}^{-1}$	STD	Dry biomass weight $\text{g m}^{-2}$	STD	Hg mass $\mu\text{g m}^{-2}$	STD
Belowground	Live Root	171.7	111.9	361	114	70.0	63.7
	Live Rhizome	37.3	13.6	792	231	38.1	22.4
	Live Root and Rhizome	84.6	49.1	1,153	321	108.1	83.4
	Senesced Biomass	385.9	224.2	11,724	1,165	4,116.1	1,141.0
	Mineral and Humus	172.7	140.8	112,439	-	21,350.9	-
	Bulk Soil	202.1	117.8	125,316	25,475	25,575.1	14,408.7
Aboveground	Green Biomass	16.2	2.0	368	149	5.7	2.1
	Senesced Biomass	15.2	2.2	215	92	3.3	1.7
	Green and Senesced	-	-	583	208	9.0	3.3

39

Table S3. Hg isotope signatures in salt marsh plant tissues and soils and their corresponding Hg concentrations.

Item	Sample ID	THg concentration (ng g <sup>-1</sup> )	$\delta^{202}\text{Hg}$ (‰)	$\Delta^{200}\text{Hg}$ (‰)	$\Delta^{199}\text{Hg}$ (‰)	$\Delta^{201}\text{Hg}$ (‰)
Aboveground biomass	ABO-L-1	4.6	-1.07	0.11	0.20	0.16
	ABO-L-2	8.0	-1.61	0.06	0.43	0.26
	ABO-L-3	6.9	-1.21	0.07	0.42	0.23
	ABO-L-4	7.9	-1.29	0.04	0.32	0.11
Rhizome	BL-RHI-1	28.7	-0.70	-0.03	0.16	-0.02
	BL-RHI-2	35.0	-1.31	0.04	0.13	0.08
	BL-RHI-3	18.0	-0.80	0.02	0.15	0.11
	BL-RHI-4	36.5	-1.41	-0.05	0.22	0.09
Root	BL-ROOT1	52.4	-0.69	0.04	0.20	0.06
	BL-ROOT2	138.0	-0.75	0.04	0.22	0.08
	BL-ROOT3	93.0	-0.66	0.02	0.13	0.03
	BL-ROOT3-2	93.0	-0.73	0.01	0.14	0.01
	BL-ROOT4	308.6	-0.69	-0.01	0.11	0.07
Surface Soil	S1L1	172	-0.32	0.03	0.14	0.10
	S1L2	275	-0.41	-0.02	0.16	0.02
	S1L3-4	378	-0.42	0.01	0.17	0.01
	S2L1	220	-0.36	0.05	0.17	0.11
	S2L2	429	-0.35	0.05	0.17	0.06
	S2L3-4	373	-0.29	0.03	0.16	0.06
	S3L1	119	-0.31	-0.01	0.17	0.01
	S3L1-2	119	-0.39	0.00	0.13	0.06
	S3L2	269	-0.60	0.02	0.07	0.07
	S3L3-4	406	-0.44	0.00	0.15	0.03
	S4L1	191	-0.41	-0.01	0.15	0.00
	S4L2	349	-0.41	0.03	0.20	0.03
	S4L3-4	416	-0.42	0.00	0.11	-0.02
	Deep Soil	S1L9	57	-0.51	-0.01	0.04
S2L9		56	-0.53	0.00	0.10	0.12
S3L9		9	-0.72	0.04	0.19	-0.02
S4L9		19	-0.92	0.03	-0.09	-0.13
S4L9-2		19	-0.92	0.02	-0.07	-0.12

43 **Table S4. Quality control results for certified reference materials (CRMs)**

CRM	Matrix	n	$\delta^{202}\text{Hg}$ ‰ ( $\pm 2\sigma$ )	$\Delta^{199}\text{Hg}$ ‰ ( $\pm 2\sigma$ )	$\Delta^{200}\text{Hg}$ ‰ ( $\pm 2\sigma$ )	$\Delta^{201}\text{Hg}$ ‰ ( $\pm 2\sigma$ )
MESS-4	Marine sediment	6	$-1.84 \pm 0.10$	$-0.01 \pm 0.07$	$-0.02 \pm 0.06$	$-0.08 \pm 0.07$
RM8610	UM- Almaden	16	$-0.55 \pm 0.10$	$-0.04 \pm 0.09$	$0.01 \pm 0.09$	$-0.04 \pm 0.07$

44

45

46 **Table S5. Estimated contributions of atmospheric GEM, roots and precipitation to vegetation from isotope mixing model.**

Term	Estimated Contribution (method 1)	Estimated Contribution (method 2)
Atmospheric GEM	$0.33 \pm 0.09$	$0.32 \pm 0.07$
Roots	$0.29 \pm 0.18$	$0.35 \pm 0.12$
Precipitation	$0.38 \pm 0.14$	$0.33 \pm 0.06$

47

48

49 **Table S6. Hg isotopic signatures of salt marsh plants and soils (this study) and other published data.**

Item	$\delta^{202}\text{Hg}$ (‰)		$\Delta^{199}\text{Hg}$ (‰)		$\Delta^{200}\text{Hg}$ (‰)		Reference
	Median	Min to Max	Median	Min to Max	Median	Min to Max	
Aboveground veg. (n=4)	-1.25	-1.61 to -1.07	0.37	0.20 to 0.43	0.06	0.04 to 0.11	this study
Rhizome (n=4)	-1.05	-1.41 to -0.70	0.16	0.13 to 0.22	-0.01	-0.05 to 0.04	this study
Root (n=4)	-0.69	-0.75 to -0.66	0.17	0.11 to 0.22	0.03	-0.01 to 0.04	this study
Root and rhizome (n=8)	-0.73	-1.41 to -0.66	0.16	0.11 to 0.22	0.02	-0.05 to 0.04	this study
Soil (n=16)	-0.42	-0.92 to -0.29	0.15	-0.02 to 0.20	0.01	-0.02 to 0.05	this study

Item	$\delta^{202}\text{Hg}$ (‰)		$\Delta^{199}\text{Hg}$ (‰)		$\Delta^{200}\text{Hg}$ (‰)		Reference
	Median	IQR*	Median	IQR	Median	IQR	
Upland veg. (n=120)	-2.84	-3.06 to -2.37	-0.37	-0.42 to -0.27	-0.02	-0.05 to 0.01	Review by Zhou et al., 2021
Rainfall (n=106)	-0.30	-0.63 to 0.03	0.40	0.21 to 0.52	0.17	0.11 to 0.22	Jiskra et al., 2021
Ocean sediment (n=92)	-0.85	-1.21 to -0.49	0.08	0.02 to 0.11	0.02	0.01 to 0.04	Jiskra et al., 2021
Ocean water total Hg (n=16)	-0.24	-0.42 to -0.04	0.06	0.02 to 0.01	0.02	-0.01 to 0.03	Jiskra et al., 2021
Atm Hg (n=220)	0.43	0.09 to 0.77	-0.20	-0.13 to -0.06	-0.05	-0.08 to -0.03	Jiskra et al., 2021
Industrial Hg (n=46)	-0.64	-0.72 to -0.42	0.02	-0.03 to 0.04	0.01	0.00 to 0.03	Estrade et al., 2011; Huang et al., 2016; Kwon et al., 2014; Lepak et al., 2015; Washburn et al., 2017

50 \*IQR: Inter-Quartile Range

51



52 Table S7. Hg concentrations in washed and unwashed aboveground green biomass samples.

Date	<i>S. alterniflorus</i> - unwashed		<i>S. alterniflorus</i> - washed*		Estimated throughfall ( $\mu\text{g kg}^{-1}$ )**
	Hg Concentration ( $\mu\text{g kg}^{-1}$ )	STD	Hg Concentration ( $\mu\text{g kg}^{-1}$ )	STD	
Aug-21	10.1	0.2	7.0	0.0	-
Sep-21	9.7	2.8	7.9	0.6	-
Oct-21	10.8	3.2	11.4	4.9	-
Nov-21	15.8	1.2	16.2	2.6	-
<b>Average</b>	<b>11.8</b>	<b>3.4</b>	<b>11.1</b>	<b>4.6</b>	<b>0.7</b>
Date	<i>S. pumilus</i> - unwashed		<i>S. pumilus</i> - washed*		Estimated throughfall ( $\mu\text{g kg}^{-1}$ )**
	Hg Concentration ( $\mu\text{g kg}^{-1}$ )	STD	Hg Concentration ( $\mu\text{g kg}^{-1}$ )	STD	
Aug-21	8.6	1.0	7.0	0.6	-
Sep-21	10.9	2.1	9.0	1.0	-
Oct-21	12.8	1.7	11.8	1.0	-
Nov-21	18.8	3.2	16.2	1.7	-
<b>Average</b>	<b>13.0</b>	<b>4.3</b>	<b>11.3</b>	<b>3.7</b>	<b>1.8</b>

53 \* Assumed structural Hg (not subject to throughfall).

54 \*\* Throughfall is estimated as amount of Hg washed off from aboveground tissues

55

Table S8. Comparing Hg concentrations in aboveground plants and roots with other contaminated and non-contaminated marsh vegetation.

Study sites	Plant Species	Session	THg $\mu\text{g kg}^{-1}$	Reference	Note
Piles Creek, NJ, USA	<i>S. alterniflorus</i>	Aboveground	160 $\pm$ 70.0	Kraus et al., 1986	Contamination
Hackensack Meadowlands, NJ, USA	<i>Phragmites australis</i>	Aboveground	18-30	Windham et al., 2001	Contamination
	<i>S. alterniflorus</i>		30-90		
Ria de Aveiro Coastal Lagoon, Portugal	<i>Halimione portulacoides</i>	Aboveground	88-970	Anjum et al., 2011	Contamination
	<i>Juncus maritimus</i> Collected	Root	248-9,957		
		Aboveground	23-268		
Tagus estuary, Portugal	<i>Halimione Portulacoides</i>	Aboveground	417-23,330	Canário et al., 2017	Contamination
	<i>Sarcocornia fruticosa</i>		53 $\pm$ 12		
	<i>S. maritima</i>		12 $\pm$ 7		
Tagus estuary, Portugal	<i>Halimione Portulacoides</i>	Root	23 $\pm$ 9	Canário et al., 2017	Contamination
	<i>Sarcocornia fruticosa</i>		1124 $\pm$ 21		
	<i>S. maritima</i>		873 $\pm$ 39		
Salt marsh, northern Spain	<i>Juncus maritimus</i>	Aboveground	1031 $\pm$ 42	Garcia-Ordiales et al., 2020	Contamination
		Root	58-2,522		
Yangtze River estuary, China	overall	Aboveground	12.5 $\pm$ 2.5 (9.0-17.4)	Wang et al., 2021	Contamination
	<i>S. alterniflorus</i>		10.2 $\pm$ 0.9		
	<i>P. australis</i>		12.6 $\pm$ 1.8		
	<i>S. marqueter</i>		14.7 $\pm$ 1.8		
Yangtze River estuary, China	<i>S. alterniflorus</i>	Root	36.6 $\pm$ 6.7	Wang et al., 2021	Contamination
	<i>P. australis</i>		9.9 $\pm$ 2.9		
	<i>S. marqueter</i>		34.0 $\pm$ 4.7		

57

58

59

60

61

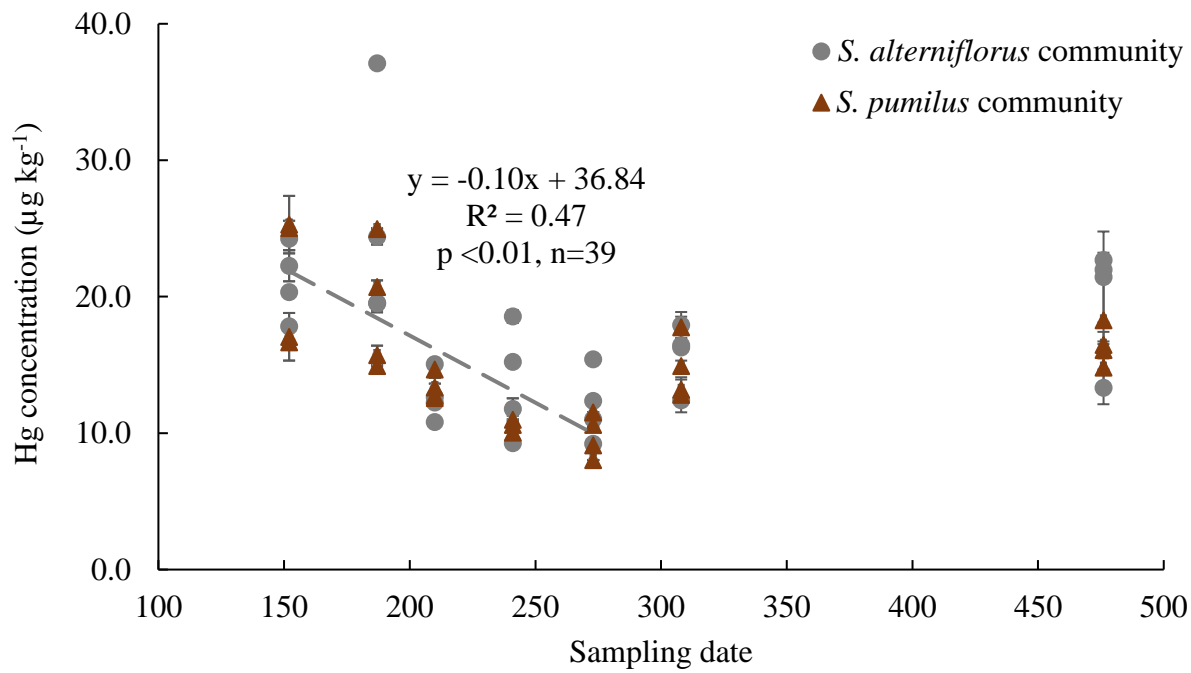
62

63 **Table S8. Comparing Hg concentrations in aboveground and roots with other contaminated and non-contaminated marsh vegetation (Continued).**

Study sites	Plant Species	Session	THg $\mu\text{g kg}^{-1}$	Reference	Note
Big Sheepshead Creek, NJ, USA	<i>S. alterniflorus</i>	Aboveground	20 $\pm$ 0	Kraus et al., 1986	No contamination
Great Bay Estuary, NH, USA	<i>S. alterniflorus</i>	Aboveground	4.61-33.4	Heller and Weber, 1998	No contamination
Ria de Aveiro Coastal Lagoon, Portugal	<i>Halimione portulacoides</i>	Aboveground	32-79	Anjum et al., 2011	No Contamination
		Root	153-802		
	<i>Juncus maritimus</i> Collected	Aboveground	3-24		
		Root	152-358		
Parker River, MA, USA	Overall (n=56)		7.6 $\pm$ 5.5* (0.8-24.0)	This study	No contamination
	<i>S. alterniflorus</i>	Aboveground	5.1 $\pm$ 3.3* (0.8-11.7)		
	<i>S. pumilus</i>		9.7 $\pm$ 6.6* (2.0-24.0)		
Parker River, MA, USA	Overall (n=4)		171.7 $\pm$ 111.9	This study	No contamination
	<i>S. alterniflorus</i>	Root	84.5 $\pm$ 47.0		
	<i>S. pumilus</i>		258.9 $\pm$ 70.3		

64 \* Range across growing season and late season maximum values

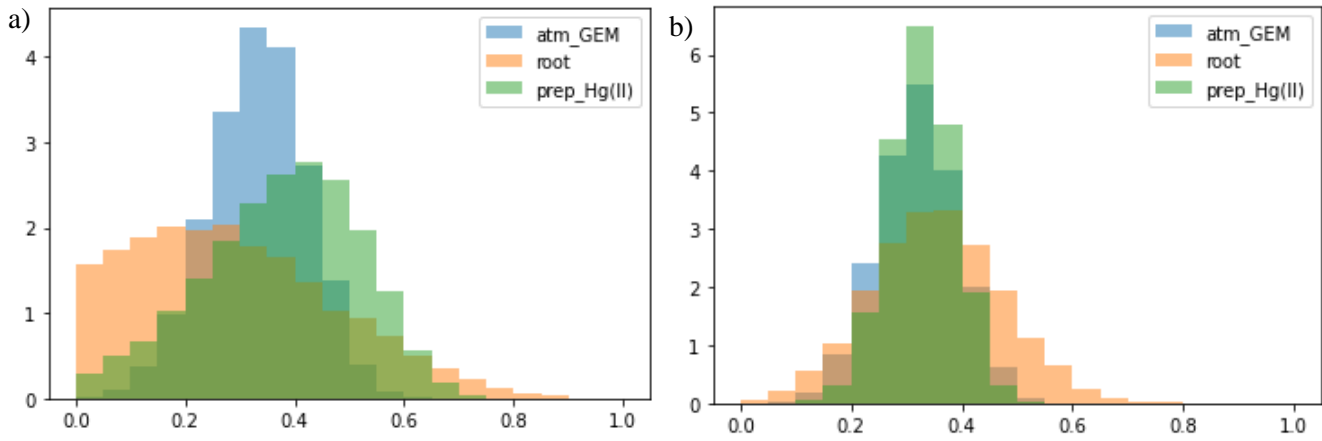
65



66

67 **Figure S1. Hg concentrations of seasonal patterns of senesced *S. alterniflorus* and *S. pumilus* communities with sampling dates in 2021.**  
 68 **Grey circles denote of senesced *S. alterniflorus* communities, and brown triangles denote of senesced *S. pumilus* communities. Standard**  
 69 **errors indicate four replicates.**

70



72

73

74

75

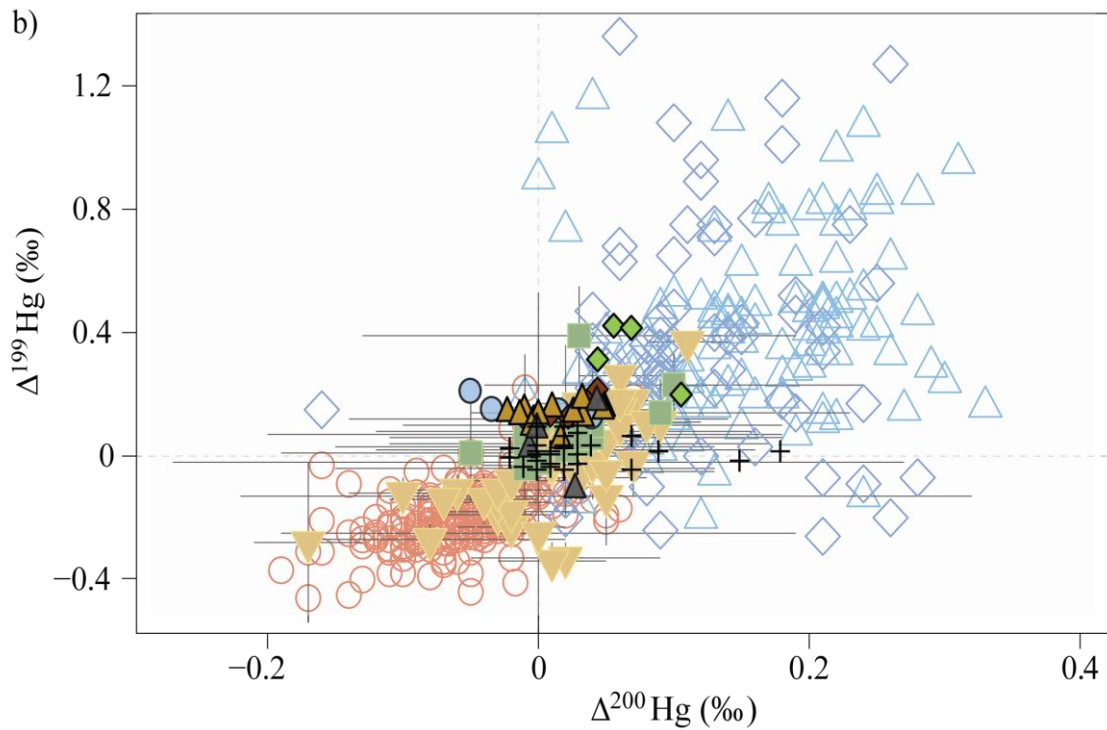
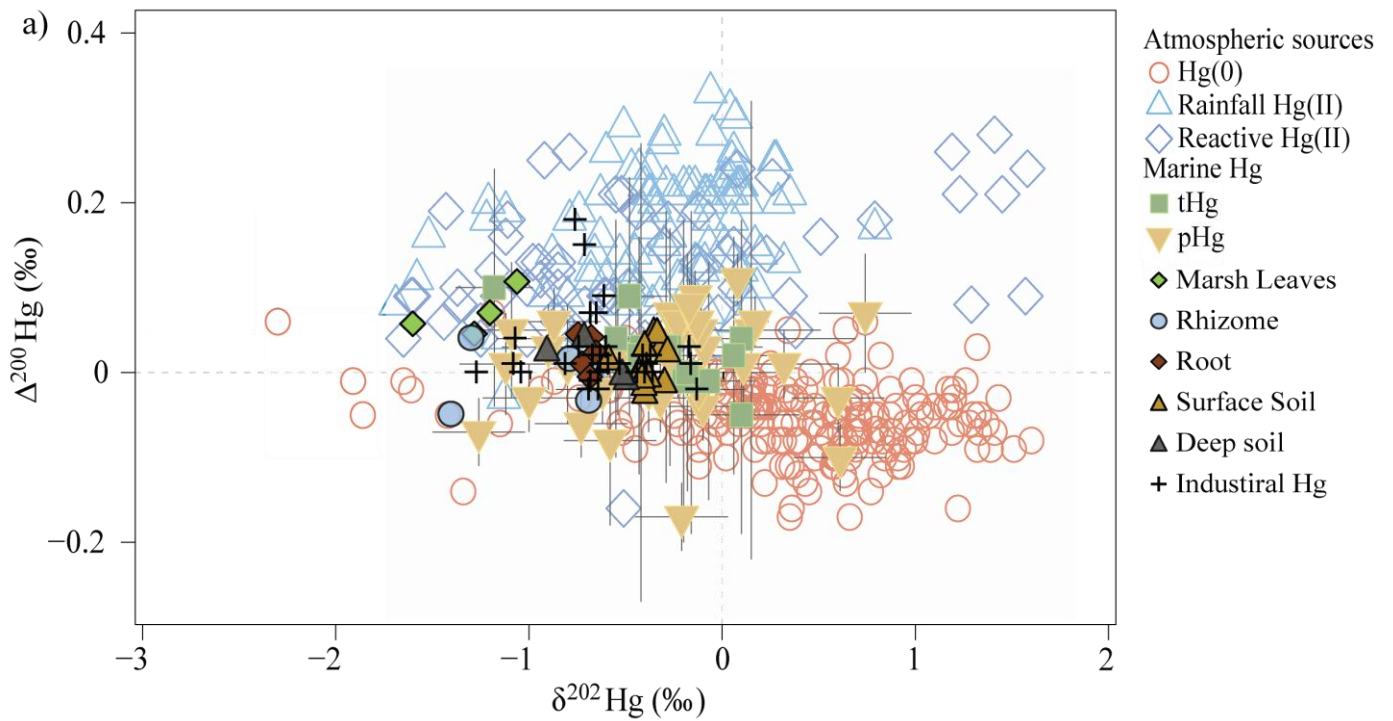
76

77

78

**Figure S2. Results of Monte Carlo trials used to simulate contribution to vegetation in an isotope mixing model, including atmospheric GEM (calculated using published terrestrial upland foliage which is dominated by atmospheric GEM sources), root samples of salt marsh plants measured in this study, and published precipitation data. Panel (a) shows results when uncertainty is specified as the mean and standard deviation of measured isotopic values in this study. Panel (b) shows results when the lowest performing certified reference material (CRM) is used to specify uncertainty in measurements. Greater variance in panel (a) reflects the limited sample sizes (n) in this study.**

79



84 **Figure S3. Relationships of  $\Delta^{202}\text{Hg}$  and  $\Delta^{199}\text{Hg}$  (a), and of  $\Delta^{200}\text{Hg}$  and  $\Delta^{199}\text{Hg}$  (b) of previous published marine Hg sources, atmospheric**  
 85 **Hg sources (Jiskra et al., 2021), industrial Hg polluted soils and sediments (Estrade et al., 2011; Huang et al., 2016; Kwon et al., 2014;**  
 86 **Lepak et al., 2015; Washburn et al., 2017), along with Hg signatures of marsh plants and soils in this study. Different color symbols**  
 87 **indicate different marsh samples.**

## 89 References

- 90 Anjum, N. A., Ahmad, I., Válega, M., Pacheco, M., Figueira, E., Duarte, A. C., and Pereira, E.: Impact of seasonal  
91 fluctuations on the sediment-mercury, its accumulation and partitioning in *Halimione portulacoides* and *Juncus*  
92 *maritimus* collected from Ria de Aveiro coastal lagoon (Portugal), *Water. Air. Soil Pollut.*, 222, 1–15,  
93 <https://doi.org/10.1007/s11270-011-0799-4>, 2011.
- 94 Canário, J., Poissant, L., Pilote, M., Caetano, M., Hintelmann, H., and O’Driscoll, N. J.: Salt-marsh plants as  
95 potential sources of Hg<sup>0</sup> into the atmosphere, *Atmos. Environ.*, 152, 458–464,  
96 <https://doi.org/10.1016/j.atmosenv.2017.01.011>, 2017.
- 97 Estrade, N., Carignan, J., and Donard, O. F. X.: Tracing and quantifying anthropogenic mercury sources in soils of  
98 northern France using isotopic signatures, *Environ. Sci. Technol.*, 45, 1235–1242, <https://doi.org/10.1021/es1026823>,  
99 2011.
- 100 Garcia-Ordiales, E., Roqueñí, N., and Loredó, J.: Mercury bioaccumulation by *Juncus maritimus* grown in a Hg  
101 contaminated salt marsh (northern Spain), *Mar. Chem.*, 226, 103859,  
102 <https://doi.org/10.1016/j.marchem.2020.103859>, 2020.
- 103 Heller, A. A. and Weber, J. H.: Seasonal study of speciation of mercury(II) and monomethylmercury in *Spartina*  
104 *alterniflora* from the Great Bay Estuary, NH, *Sci. Total Environ.*, 221, 181–188, [https://doi.org/10.1016/S0048-](https://doi.org/10.1016/S0048-9697(98)00285-X)  
105 [9697\(98\)00285-X](https://doi.org/10.1016/S0048-9697(98)00285-X), 1998.
- 106 Huang, Q., Chen, J., Huang, W., Fu, P., Guinot, B., Feng, X., Shang, L., Wang, Z., Wang, Z., Yuan, S., Cai, H., Wei,  
107 L., and Yu, B.: Isotopic composition for source identification of mercury in atmospheric fine particles, *Atmos. Chem.*  
108 *Phys.*, 16, 11773–11786, <https://doi.org/10.5194/acp-16-11773-2016>, 2016.
- 109 Jiskra, M., Heimbürger-Boavida, L.-E., Desgranges, M.-M., Petrova, M. V., Dufour, A., Ferreira-Araujo, B.,  
110 Masbou, J., Chmeleff, J., Thyssen, M., Point, D., and Sonke, J. E.: Mercury stable isotopes constrain atmospheric  
111 sources to the ocean, *Nature*, 597, 678–682, <https://doi.org/10.1038/s41586-021-03859-8>, 2021.
- 112 Kraus, M. L., Weis, P., and Crow, J. H.: The excretion of heavy metals by the salt marsh cord grass, *Spartina*  
113 *alterniflora*, and *Spartina*’s role in mercury cycling, *Mar. Environ. Res.*, 20, 307–316, [https://doi.org/10.1016/0141-](https://doi.org/10.1016/0141-1136(86)90056-5)  
114 [1136\(86\)90056-5](https://doi.org/10.1016/0141-1136(86)90056-5), 1986.
- 115 Kwon, S. Y., Blum, J. D., Chen, C. Y., Meattay, D. E., and Mason, R. P.: Mercury isotope study of sources and  
116 exposure pathways of methylmercury in estuarine food webs in the northeastern U.S., *Environ. Sci. Technol.*, 48,  
117 10089–10097, <https://doi.org/10.1021/es5020554>, 2014.
- 118 Lepak, R. F., Yin, R., Krabbenhoft, D. P., Ogorek, J. M., DeWild, J. F., Holsen, T. M., and Hurley, J. P.: Use of  
119 Stable Isotope Signatures to Determine Mercury Sources in the Great Lakes, *Environ. Sci. Technol. Lett.*, 2, 335–  
120 341, <https://doi.org/10.1021/acs.estlett.5b00277>, 2015.
- 121 Wang, Y., Wang, Z., Zheng, X., and Zhou, L.: Influence of *Spartina alterniflora* invasion on mercury storage and  
122 methylation in the sediments of Yangtze River estuarine wetlands, *Estuar. Coast. Shelf Sci.*, 265, 107717,  
123 <https://doi.org/10.1016/j.ecss.2021.107717>, 2021.
- 124 Washburn, S. J., Blum, J. D., Demers, J. D., Kurz, A. Y., and Landis, R. C.: Isotopic Characterization of Mercury

125 Downstream of Historic Industrial Contamination in the South River, Virginia, *Environ. Sci. Technol.*, 51, 10965–  
126 10973, <https://doi.org/10.1021/acs.est.7b02577>, 2017.

127 Weis, J. S. and Weis, P.: Metal uptake, transport and release by wetland plants: implications for phytoremediation  
128 and restoration, *Environ. Int.*, 30, 685–700, <https://doi.org/10.1016/j.envint.2003.11.002>, 2004.

129 Windham, L., Weis, J. S., and Weis, P.: Patterns and processes of mercury release from leaves of two dominant salt  
130 marsh macrophytes, *Phragmites australis* and *Spartina alterniflora*, *Estuaries*, 24, 787–795,  
131 <https://doi.org/10.2307/1353170>, 2001.

132 Windham, L., Weis, J. ., and Weis, P.: Uptake and distribution of metals in two dominant salt marsh macrophytes,  
133 *Spartina alterniflora* (cordgrass) and *Phragmites australis* (common reed), *Estuar. Coast. Shelf Sci.*, 56, 63–72,  
134 [https://doi.org/10.1016/S0272-7714\(02\)00121-X](https://doi.org/10.1016/S0272-7714(02)00121-X), 2003.

135 Zhou, J., Obrist, D., Dastoor, A., Jiskra, M., and Ryjkov, A.: Vegetation uptake of mercury and impacts on global  
136 cycling, *Nat. Rev. Earth Environ.*, 2, 269–284, <https://doi.org/10.1038/s43017-021-00146-y>, 2021.

137